Electronic Supplementary Information

Molecular Insights into the Resistance of Phospholipid Heads to Membrane Penetration of Graphene Nanosheets

Zhen Li,[a] Xiaohong Zhu,[b] Jiawei Li,[ac] Jie Zhong,[d] Jun Zhang,[a] and Jun Fan*[b]*

[a] School of Materials Science and Engineering, China University of Petroleum (East China), Qingdao 266580, China. E-mail: zhangjun.upc@gmail.com

[b] Department of Materials Science and Engineering, City University of Hong Kong, Kowloon 999077, Hong Kong, China. E-mail: junfan@cityu.edu.hk

[c] Key Laboratory of Marine Environmental Corrosion and Bio-Fouling, Institute of Oceanology, Chinese Academy of Sciences, Qingdao 266071, China.

[d] Department of Earth and Environmental Science and Department of Chemistry, University of Pennsylvania, Philadelphia, PA, 19104-6316, USA

CONTENTS

S1. Interaction State Analysis

Starting from different orientations, the nanosheet interplays with the phospholipid bilayer and gradually evolves into equilibrated interaction states. As shown in Fig. 1b in the main text, three typical interaction states were observed, including “adhering”, “penetrating”, and “departing”. We considered different initial nanosheet orientations using characteristic angles ϑ and φ as shown in Fig. 1a in the main text, and performed 10 simulation replicas for each orientation (totally 130 MD simulations).

To quantitatively determine the final interaction state of each model and evaluate the probability of formation of the three interaction states (listed in Fig. 1c in the main text), we traced the position and the orientation of the nanosheet. The nanosheet position is defined as the distance, d, from the bilayer surface to the nearest atom of the nanosheet; the nanosheet orientation is defined as the angle, α, between the normal vector of the nanosheet plane and z axis. With tracing temporal evolution of d and α,

- once d became larger than 15 Å, we would designate that the nanosheet has departed from the nanosheet-membrane interface and stop the simulation, and the final state is “state C: departing”;
- if d is slightly larger than 0 Å and α converges to around 0 degree, the nanosheet adheres onto the bilayer surface, and the final interaction state is “state A: adhering”;
- greatly decreased d value and converged α to large values (near 90 degree) means that the nanosheet penetrates the bilayer, and the interaction state is “state B: penetrating”.

According to above three criteria, we analyzed the 130 MD trajectories, and determined the result shown in Fig. 1c in the main text. Fig. S1-S5 present temporal evolution of d and α, as well as the verdict of interaction state for all 130 models.

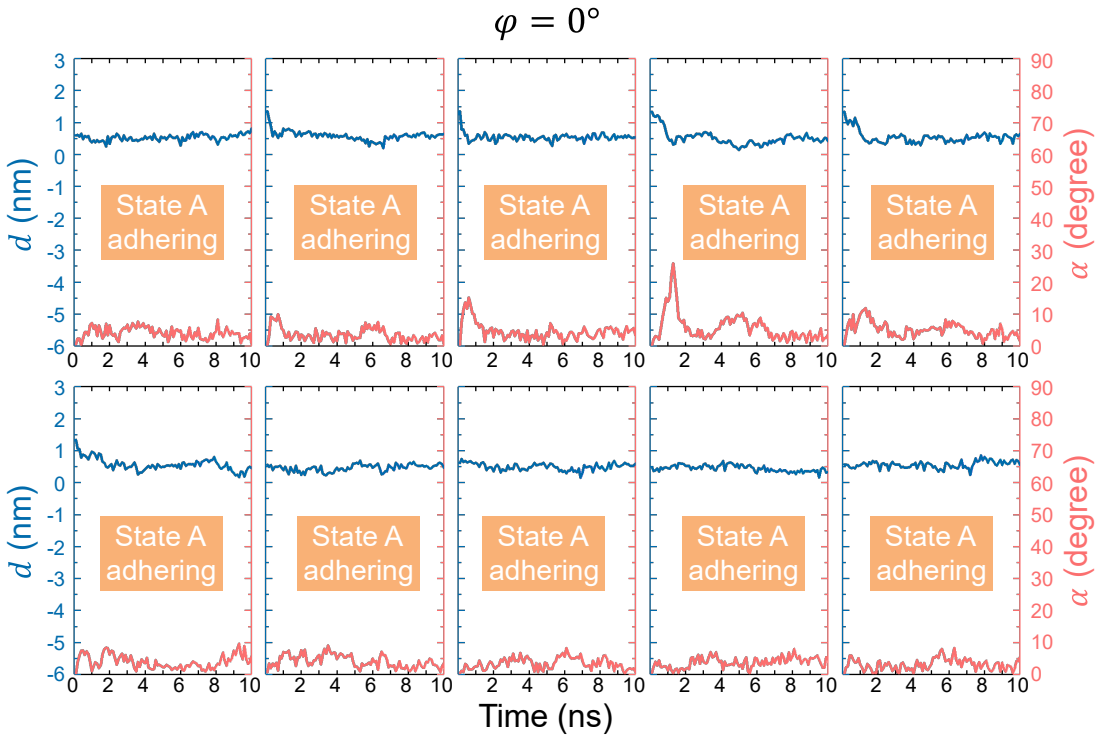

Fig. S1 Temporal evolution of nanosheet position and orientation, as well as verdict of the final interaction state, for initial models with φ = 0°.

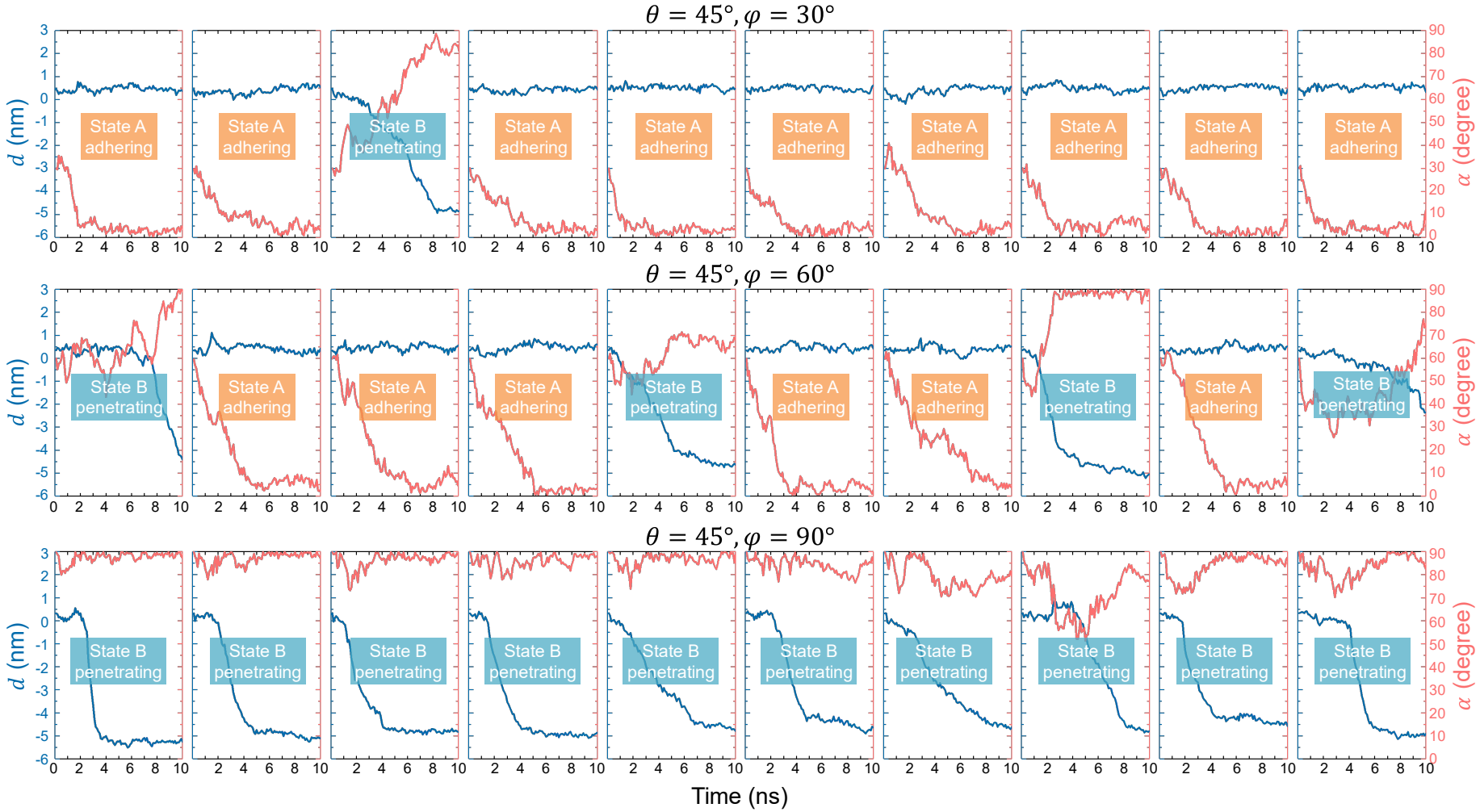

Fig. S2 Temporal evolution of nanosheet position and orientation, as well as verdict of the final interaction state, for initial models with ϑ = 45° and φ = 30°, 60°, 90°.

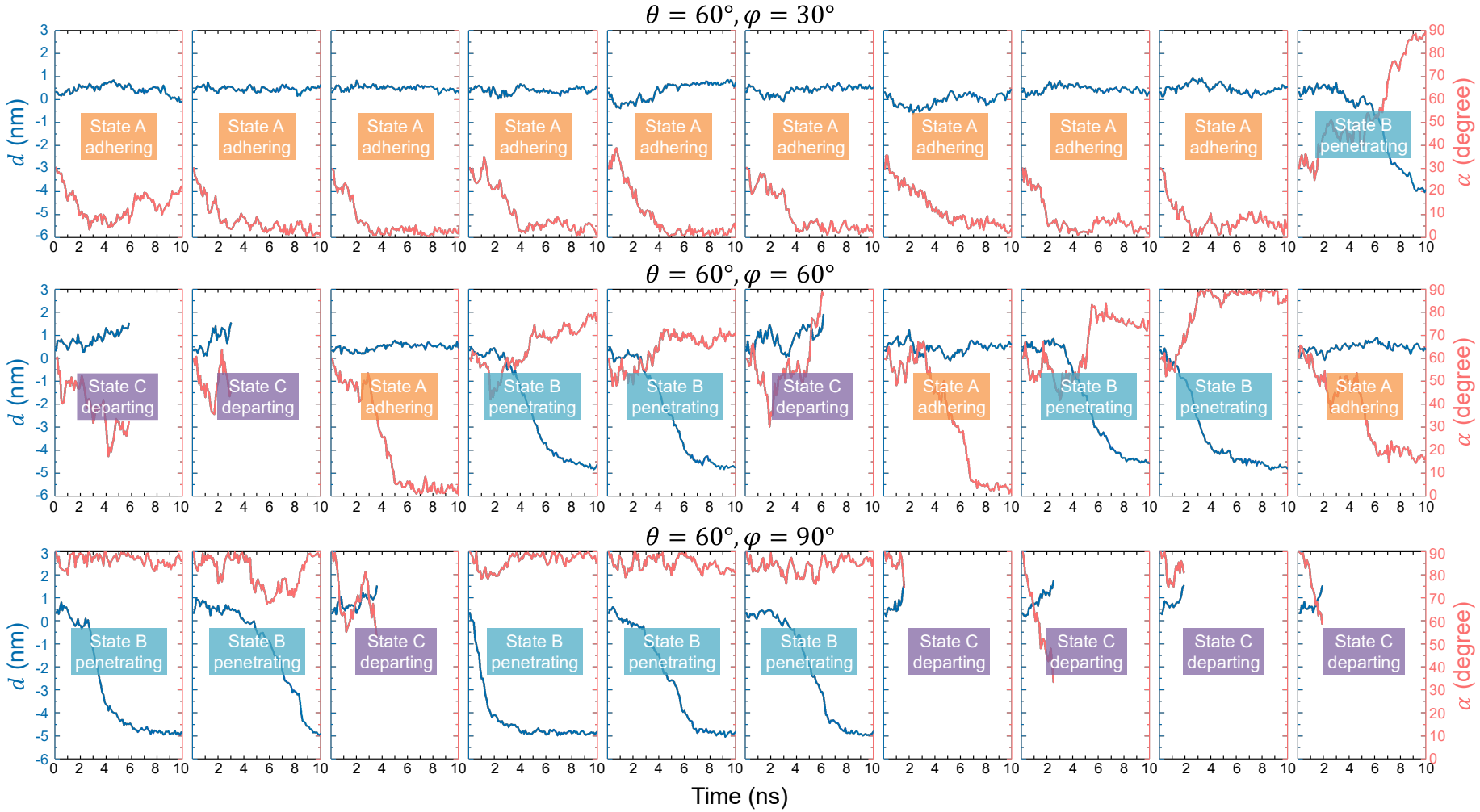

Fig. S3 Temporal evolution of nanosheet position and orientation, as well as verdict of the final interaction state, for initial models with ϑ = 60° and φ = 30°, 60°, 90°.

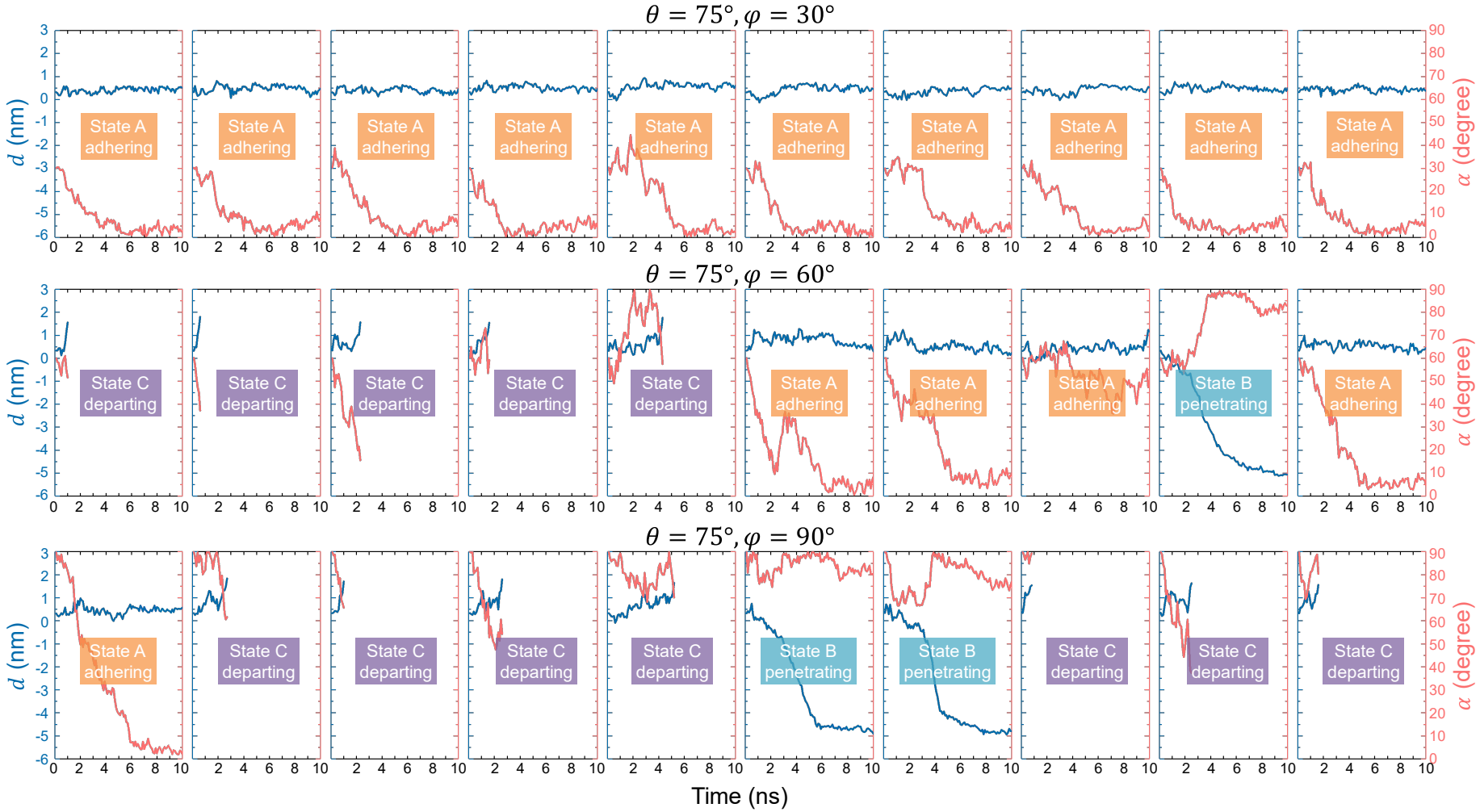

Fig. S4 Temporal evolution of nanosheet position and orientation, as well as verdict of the final interaction state, for initial models with ϑ = 75° and φ = 30°, 60°, 90°.

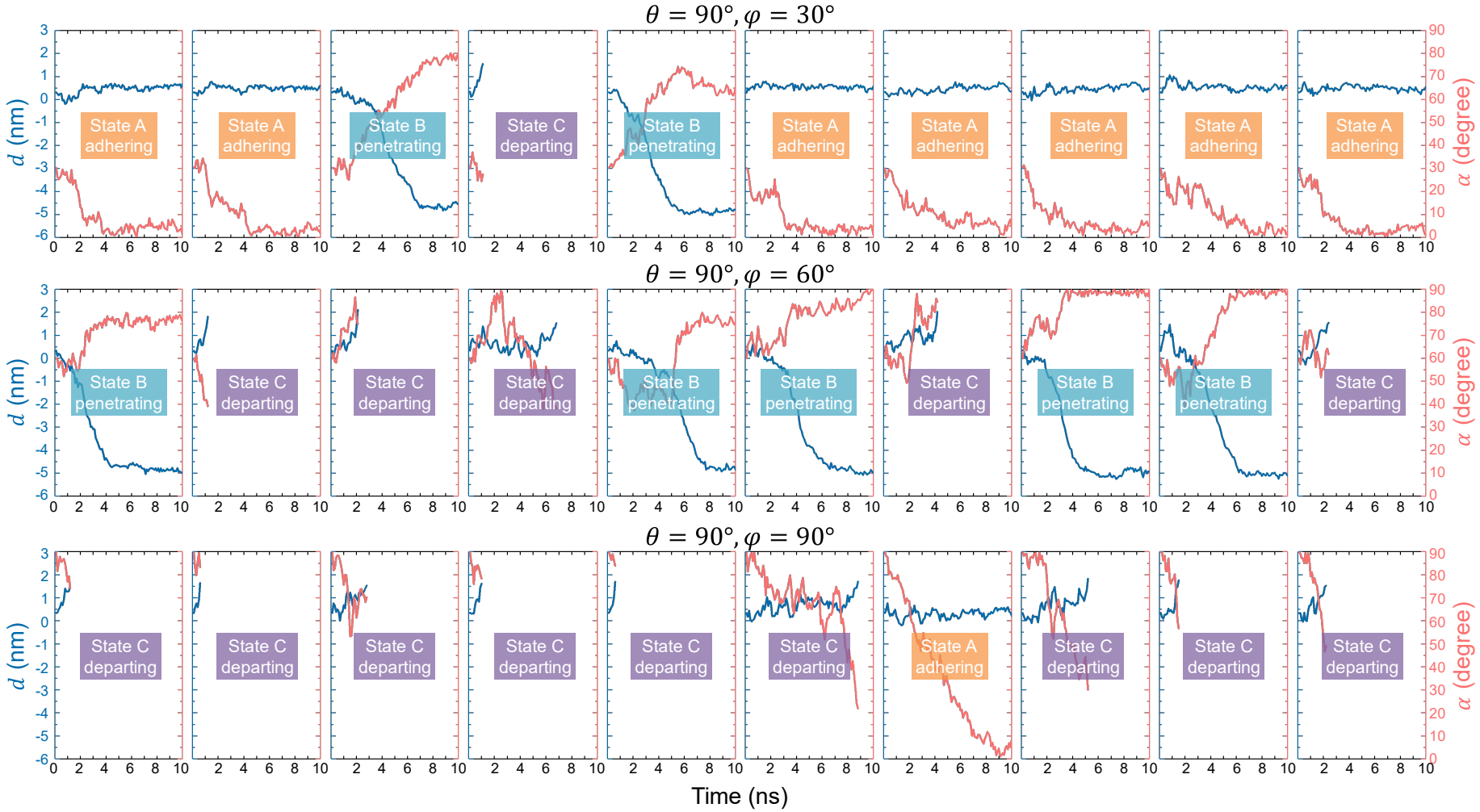

Fig. S5 Temporal evolution of nanosheet position and orientation, as well as verdict of the final interaction state, for initial models with ϑ = 90° and φ = 30°, 60°, 90°.

S2. Penetration Pathway Analysis

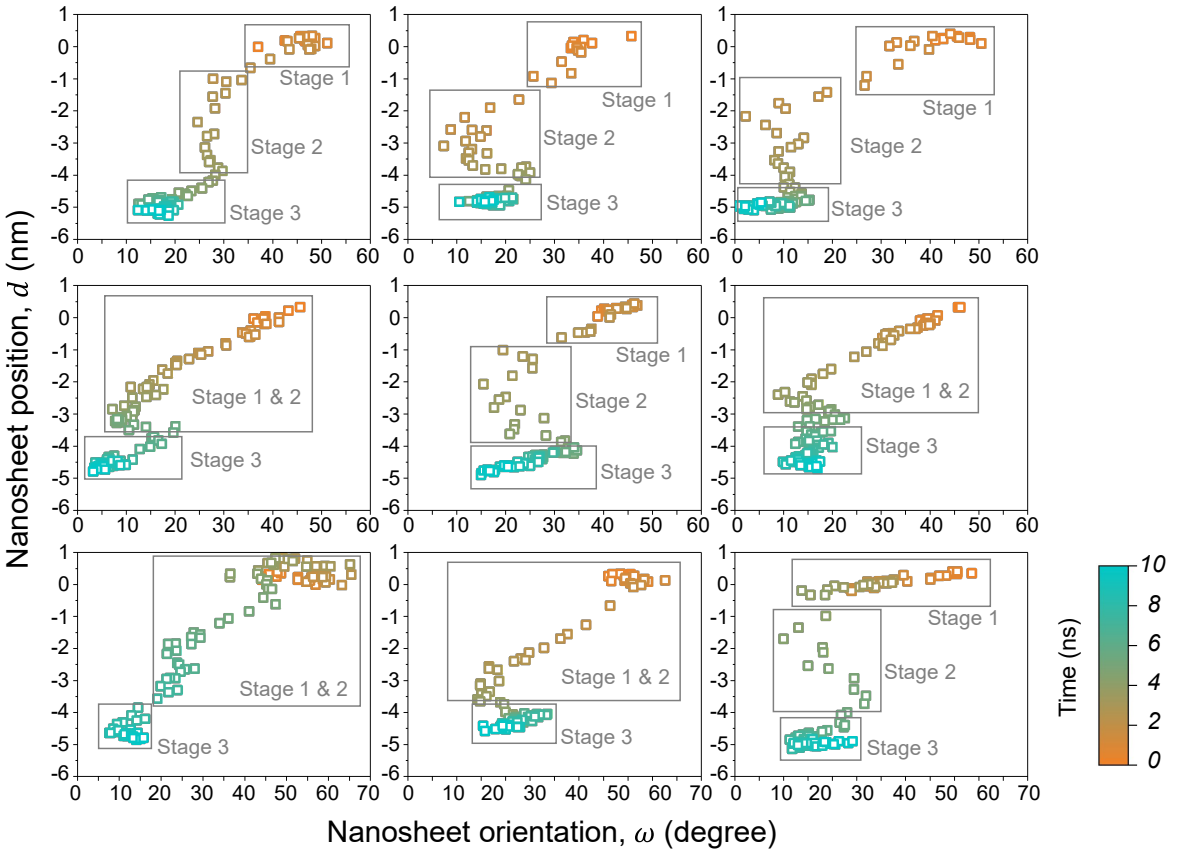

Fig. S6 Temporal evolution of the distance from the bilayer surface to the bottom of the nanosheet and the angle between diagonal axis of the nanosheet and z axis, for additional 9 independent models with the edge-approaching orientation.

S2.1 Corner-first penetration

As shown in Fig. 2a in the main text and movie in the Supporting Information, after approaching the lipid bilayer with one nanosheet edge, the nanosheet first rotates to wedge itself into lipid heads using its sharp corner, and then penetrates lipid tails quickly. This pathway can be quantitatively described using two parameters: the distance from the bilayer surface to the bottom of the nanosheet (d) and the angle between diagonal axis of the nanosheet and z axis (ω).

We performed 10 independent MD simulations for the edge-approaching orientation of the nanosheet. With projecting evolved d and ω to a 2D map for all the 10 simulations, we can segment the penetration process into three stages: rotating, penetrating, and relaxing.

Results of one simulation is shown in Fig. 2b in the main text, Fig. S6 here shows results of additional 9 simulations.

As shown in Fig. S6, the degree of the rotating and wedging in stage 1 varies slightly, which is a random process dominated by distribution and configuration of phospholipids nearby the nanosheet. However, all 10 simulations demonstrate that pointing to the bilayer with corner is prerequisite of the penetration. Sometimes, stage 1 and 2 are connected without obvious gap.

S2.2 Difference between the corner-first penetration and the departing of corner-approaching nanosheets

Here, although the nanosheet approaches the phospholipid bilayer with its edge, its corner is needed to penetrate the bilayer. But as shown in Fig. S4 and S5, approaching the phospholipid bilayer with the nanosheet corner cannot trigger the penetration. The difference between the two scenarios is on the position of the nanosheet corner. Barely touching the bilayer surface with the nanosheet corner is inadequate for further penetration. Penetration requires that the nanosheet corner has preliminarily inserted and interacted well with phospholipids, this can be achieved through the stage 1 of edge-approaching nanosheets (Fig. S6). Thus, touching phospholipid membrane with nanosheet edges is prerequisite of starting the penetration, and nanosheet corners facilitates the following penetration process.

S3. Umbrella Sampling

Using umbrella sampling,[1-3] we calculated potential of mean force (PMF) profiles for the nanosheet edge and corner along the normal direction of the bilayer, as shown in Fig. 4d and 4e. To evaluate the free energy barrier of penetration for both the nanosheet edge and the nanosheet corner, we applied position restraint to a row of nanosheet atom along x and y axes in umbrella sampling. Phosphorus atoms of phospholipids were position restrained along z axis to avoid the interference of membrane fluctuation during umbrella sampling.

The interval of umbrella sampling windows is 1.2 Å. In each window, distance between the nanosheet and the bilayer was restrained with harmonic force constant of 2000 $kJ \cdot mol^{-1} \cdot nm^{-2}$. Each window was simulated for 20 ns, and weighted histogram analysis method (WHAM)[2] was used to obtain PMF profiles. Fig. 4d in the main text shows PMF profiles of the nanosheet edge, here PMF profiles of the nanosheet corner is supplemented (Fig. S7). Data in Fig. 4e are derived from Fig. 4d and Fig. S7.

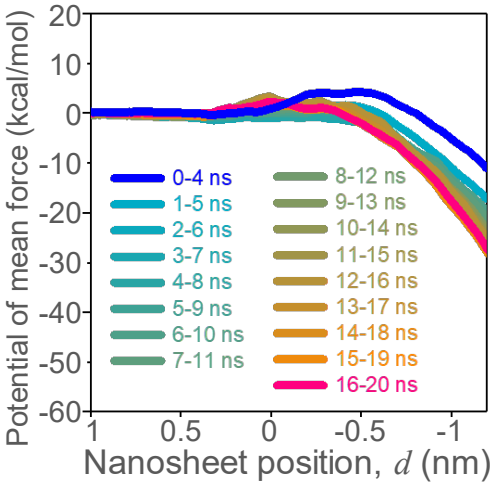

Fig. S7 Potential of mean force profile for penetration of the nanosheet corner along the normal direction of the bilayer.

S4. Steered MD Simulation for Evaluating Penetration Resistance

To evaluate the resistance of different kinds of phospholipids, and based on that, to reveal mechanisms underlying the resistance, we carried out steered MD simulations. As shown in Fig. S8, a harmonic potential with force constant of 4000 kJ·mol^{-1}·nm^{-2} is applied to the nanosheet and the reference position moves towards the bilayer with velocity of 1 nm/ns. Thus, the nanosheet is steered towards the bilayer, and the pulling force can be obtained to reflect the resistance of phospholipids to the nanosheet edge. Pulling force was outputted every 10 ps, running average with interval of 100 ps was used to obtain smoothed force profiles. As shown in Fig. 5b in the main text, the largest absolute value of pulling force is the penetration resistance (PR).

For PA, PC, PE, PG, PI, and PS bilayers, five independent steered MD simulations were carried out, and pulling force profiles were collected to obtain averaged PR (Fig. 5c in the main text). All pulling force profiles with PR values are listed in Fig. S9.

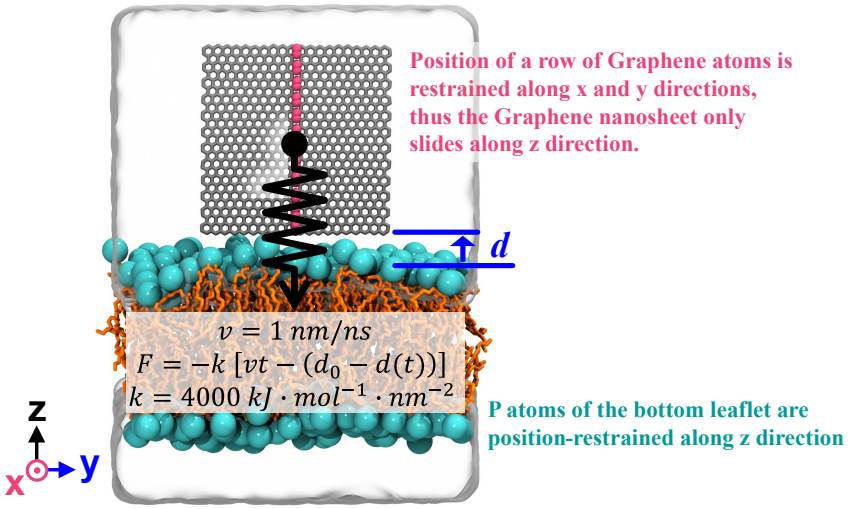

Fig. S8 Protocol of steered MD simulation for evaluating resistance of different phospholipid heads to the penetration of the nanosheet edge (Fig. 5bc in the main text).

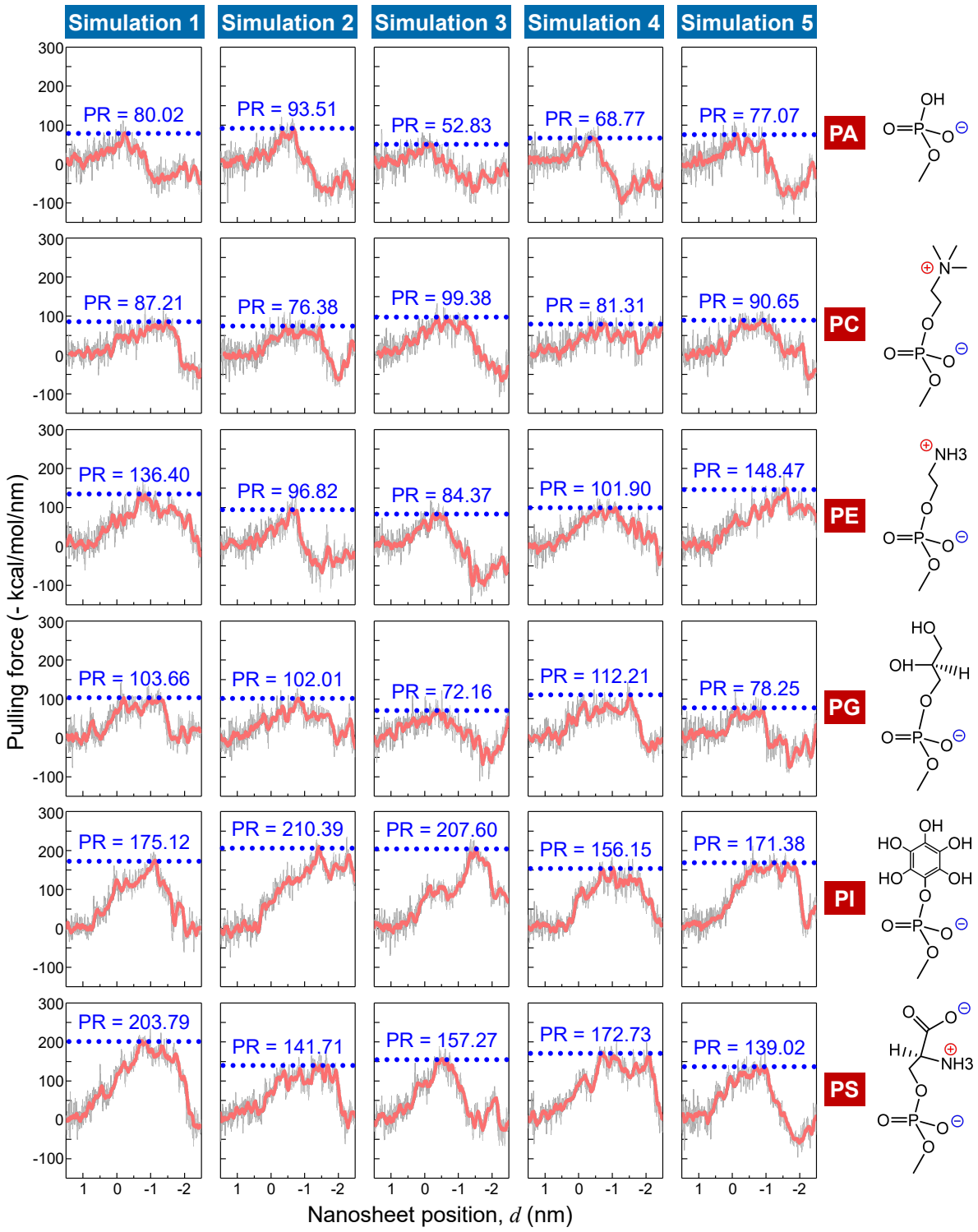

Fig. S9 Penetration resistance (PR) of different phospholipid heads to the nanosheet edge. Five independent steered MD simulations were performed for each kind of phospholipid bilayer.

S5. Interaction State Changes with Varying Phospholipid Heads

As shown in Fig. S9 and Fig. 5c in the main text, the resistance to the penetration of nanosheets is sensitive to phospholipid head types. In particular, PI and PS generate considerable barrier. To further clarify the effect of phospholipid heads, we performed unrestrained MD simulations for visualizing the destiny of the graphene nanosheet when approaching different kinds of phospholipid bilayers as listed in Fig. S9.

We know that the graphene nanosheet 100% penetrates the PC bilayer starting from the edge-approaching orientation (an edge perpendicularly points to the bilayer plane in the initial model, ϑ = 45°, φ = 90°) in our 10 independent simulations, as shown in Fig. S2. Compared with PC, larger resistances of PI and PS should reduce the probability of penetration. Thus, all our models in this part started from the edge-approaching orientation (ϑ = 45°, φ = 90°), and 10 independent simulations were carried out for PA, PE, PG, PI, and PS bilayers. Results are shown in Fig. S10.

Within our simulation replica, the penetration probability is 100% for PA and PC, 90% for PE, 80% for PG, 20% for PI, and 0% for PS bilayers. The change of interaction state is generally consistent with the PR analyses (Fig. S9).

Fig. S10 Initiating from the orientation ϑ = 45° and φ = 90°, temporal evolution of nanosheet position and orientation, as well as verdict of the final interaction state, when the graphene nanosheet interacts with C16:0-18:1 (a) PA, (b) PE, (c) PG, (d) PI, and (e) PS bilayer. 10 independent simulations were performed for each kind of phospholipid bilayer.

S6. Correlation between Penetration Resistance and Phospholipid Membrane Properties

To explain the difference of PR for PA, PC, PE, PG, PI, and PS (Fig. 5c in the main text), we carried out correlation analysis between PR and properties of lipid bilayers. The penetration resistance results from the upper layer of phospholipid heads, thus structure and dynamics of the head layer were analyzed.

First, the lateral diffusion of phospholipid heads was evaluated. As shown in Fig. S11, the mean square displacement (MSD) shows that PE heads possess the highest lateral mobility and PA>PG>PC>PS>PI. Diffusion coefficients were calculated through linearly fitting MSD profiles within [3 ns, 7 ns]. The correlation coefficient between PR and the diffusion coefficient of phospholipid heads is -0.37 (Fig. 6a in the main text), demonstrating that the resistance of phospholipid heads to the penetration of nanosheets is weakly correlated with diffusivity of phospholipids.

Structural characteristics including the thickness of phospholipid heads and the lateral area per phospholipid were analyzed. The thickness of phospholipid heads was derived from the density profile of phospholipid heads along the normal direction of the bilayer (Fig. S12), density of 1 kg/m^3 was taken as a critical value to determine the distribution range of phospholipid heads. Correlation coefficient of 0.039 (Fig. 6b in the main text) and -0.097 (Fig. 6c in the main text) demonstrate low correlation between PR and the two structural parameters.

In addition, we calculated interaction energy of phospholipid heads and counter ions in models containing 32 phospholipids in both leaflets and 64 sodium ions for PA, PG, PI, and PS bilayers. The correlation coefficient between the interaction energy and the PR value is -0.631 (Fig. 6d in the main text), which indicates that strong head-head interaction could introduce penetration barrier to some extents. However, the correlation is not that strong.

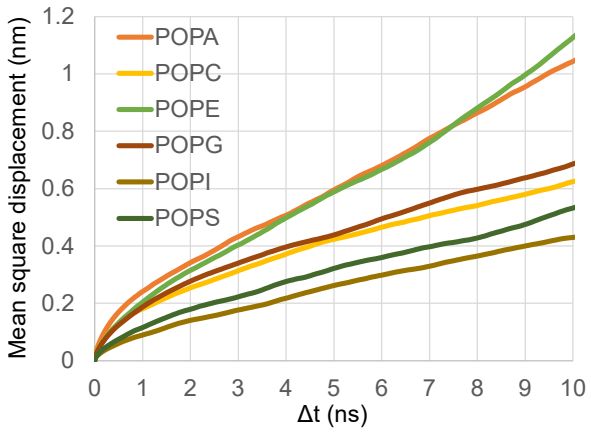

Fig. S11 Lateral mean square displacement (MSD) of phospholipids in different bilayers. MSD data were obtained by tracing position of phosphorus atoms in bilayers, and diffusion coefficient was obtained with fitting MSD profiles from 3 ns to 7 ns.

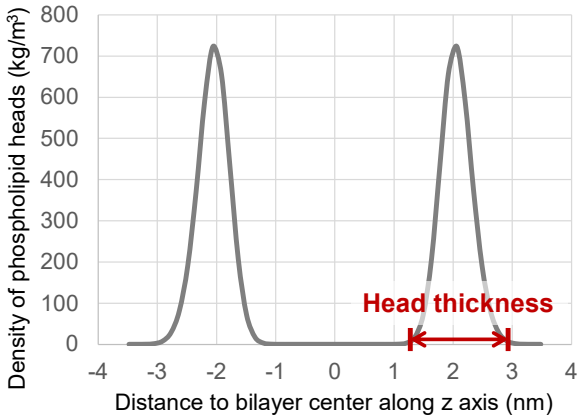

Fig. S12 Density profile of phospholipid heads (taking POPC as an example) along the normal direction of the bilayer, quantifying thickness of head layer of phospholipids. Critical density of 1 kg/m^3 was used to determine the range of head thickness.

S7. Motion Association of Adjacent Phospholipid Heads

As shown in Fig. 6e in the main text, adjacent POPS molecules are associated with each other and they move in lockstep, which may explain the large resistance of PS to the penetration of nanosheet (please see discussion in the main text). To confirm the relationship between PR and the migration style of phospholipids, we parameterized the degree of motion association of adjacent phospholipids.

The following steps were conducted to calculate the motion association of adjacent phospholipids:

- *Step 1: For each frame (2000 frames in total for 200 ns simulation in equilibrium state), randomly pick one phospholipid (phospholipid A), and find the nearest phospholipid B. Position of phosphorus atom was used to determine distance between phospholipids.*
- *Step 2: Recording x and y position in following 10 frames for phospholipid A and B, we obtain x(A1, A2, …, A10), y(A1, A2, …, A10), x(B1, B2, …, B10), and y(B1, B2, …, B10).*
- *Step 3: Calculating the motion association of adjacent phospholipids that defined as*

$$\rho = \frac{1}{2}\left(\rho_{x(A)x(B)} + \rho_{y(A)y(B)}\right) = \frac{1}{2}\left(\frac{Cov\left(x(A),x(B)\right)}{\sigma_{x(A)}\sigma_{x(B)}} + \frac{Cov\left(y(A),y(B)\right)}{\sigma_{y(A)}\sigma_{y(B)}}\right)$$

  where $Cov\left(x(A),x(B)\right)$ means covariance of variable *x*(*A1, A2, …, A10*) and *x*(*B1, B2, …, B10*); $Cov\left(y(A),y(B)\right)$ means covariance of variable *y*(*A1, A2, …, A10*) and *y*(*B1, B2, …, B10*); $\sigma_{x(A)}$ means standard deviation of *x*(*A1, A2, …, A10*); $\sigma_{x(B)}$ means standard deviation of *x*(*B1, B2, …, B10*); $\sigma_{y(A)}$ means standard deviation of *y*(*A1, A2, …, A10*); $\sigma_{y(B)}$ means standard deviation of *y*(*B1, B2, …, B10*).

- *Step 4: Repeating Step 1-3 for all frames and averaging results of ρ, to obtain the motion association of adjacent phospholipids shown in Fig. 6f (horizontal axis) in the main text.*

Results in Fig. 6f in the main text demonstrates that the motion association of adjacent phospholipids, reflecting the migration style of phospholipids in different bilayers, correlates

well with the resistance of phospholipid heads to the penetration of nanosheets (PR) with correlation coefficient of 0.96.

REFERENCES

1. B. Roux, *Comput. Phys. Commun.*, 1995, **91**, 275-282.
2. S. Kumar, J. M. Rosenberg, D. Bouzida, R. H. Swendsen and P. A. Kollman, *J. Comput. Chem.*, 1995, **16**, 1339-1350.
3. G. M. Torrie and J. P. Valleau, *J. Comput. Phys.*, 1977, **23**, 187-199.